Proceedings of the 18th UK Heat Transfer Conference
9-11 September 2024, Birmingham
UKHTC2024-30

Proceedings of Extended Abstract

DNS of Magnetohydrodynamic Rayleigh-Bénard Convection with Applications in Fusion Thermal Hydraulics

Jake Ineson[1*], Alex Skillen[1], Aleksander Dubas[2]

[1]School of Engineering, University of Manchester, Oxford Road, Manchester M13 9PL, United Kingdom

[2]Computing Division, UK Atomic Energy Authority, Culham Campus, Abingdon, OX14 3DB, United Kingdom

1. ABSTRACT

Direct numerical simulation of incompressible, inductionless magnetohydrodynamic Rayleigh-Bénard convection is conducted for Rayleigh numbers up to 10^6, a Prandtl number of 1 and for a range of Hartmann numbers in the interval $0 < Ha < 64$. First- and second- order statistics are collected for the velocity, temperature and electrical current, forming a high-resolution DNS database. The resolution of these results is ensured post-simulation by comparing the mesh-spacing and time-step with Kolmogorov length- and time- scales respectively. The Nusselt number is computed as a function of the Hartmann number, quantifying the heat transfer performance of this flow. A negative trend is observed between the Nusselt and Hartmann numbers.

2. INTRODUCTION

A promising path to commercially viable fusion energy is through harnessing power from the fusion of deuterium and tritium nuclei. Deuterium is an abundant isotope of hydrogen, but tritium rarely exists in nature. Therefore, future fusion plants such as the Spherical Tokamak for Energy Production (STEP) will produce their own tritium through the use of breeder blankets. The design of breeder blankets comes with a number of significant engineering challenges; blankets are exposed to significant temperature gradients whilst also receiving significant irradiation by neutrons. Many designs of breeder blankets involve using liquid lithium as the breeding material. A challenge for these designs is the interaction between the flow phenomena and the strong magnetic fields present in fusion. Significant magnetohydrodynamic (MHD) effects are present in liquid metal blankets, which lead to a pressure drop in the fluid as well as a degradation of the heat transfer performance, resultingly reducing overall plant efficiency. Significant work, both experimentally and in modelling, is needed to accurately quantify these effects and to help aid in the design of the fusion plants of the future. We note that experimental campaigns are challenging due to the lack of transparency of liquid metals to visible wavelengths of light, thereby preventing the use of optical flow diagnostic techniques.

This work investigates the direct numerical simulation of fusion-relevant flow physics and aims to lay the groundwork in quantifying the interaction between heat-transfer phenomena and MHD effects. The case selected is the Rayleigh-Bénard convection (RBC) of conducting fluids flowing through a magnetic field.

Significant work has already been done simulating RBC without MHD effects, due to the prevalence of such flows both in nature and in industry; notably the nuclear fusion industry. For examples, [1] provides a DNS reference for values of the Rayleigh number up to 10^7 and a Prandtl number of 0.7, whilst [2] conducts a similar study for fluids of Prandtl number 0.025. However, there is little research into RBC with MHD effects. A similar example is [3], which simulates channel flow through a magnetic field where temperature acts as a passive scalar. However, this study ignores buoyancy forces, limiting its relevance for fusion systems. There is also an example [4], which studies RBC with MHD effects using a RANS model but due to the lack of DNS research, such models are difficult to validate. So, the motivation for this study is to provide a high-resolution DNS reference dataset for MHD RBC.

3. METHDOLOGY

Natural convection of a conducting fluid in a laterally unbounded Rayleigh-Bénard cell is studied. Buoyancy-driven flow occurs between two horizontal plates which are held at fixed temperatures. The spatial and temporal variations of the velocity, temperature and electrical current in the cell are described by the inductionless MHD equations, with the addition

*Jake Ineson: jake.ineson@postgrad.manchester.ac.uk

of a Boussinesq forcing term to account for density. The relevant dimensionless parameters for this type of flow are the Rayleigh, Prandtl and Hartmann numbers

$$Ra = \frac{g\beta\Delta T H^3}{\nu} \qquad Pr = \frac{\nu}{\alpha} \qquad Ha = B_0 L \sqrt{\frac{\sigma}{\mu_0}} \qquad (1)$$

where H is the height of the Rayleigh-Bénard cell, ΔT is the temperature difference between the walls, B_0 is the applied magnetic field strength, g is the gravitational constant and μ_0 is the permeability of free space. The thermal expansion coefficient, thermal diffusivity, kinematic viscosity and electrical conductivity are given by β, α, ν and σ respectively. Only constant, uniform, wall-normal magnetic fields are considered, $\boldsymbol{B} = B_0\hat{\boldsymbol{y}}$. The velocity and time of the system are non-dimensionalised the freefall velocity, $U_{ff} = \sqrt{g\beta\Delta T H}$, and the large eddy turnover time, respectively.

The MHD equations are solved using Incompact3d [5], which discretizes the domain as a cartesian grid with stretching in the wall-normal direction. A sixth-order compact finite difference scheme is adopted for the spatial discretization whilst a third-order Adams-Bashford method is used to advance the solutions in time.

No-slip, constant temperature and electrically insulating boundary conditions are enforced at the two walls whilst the remaining directions have periodic boundaries. The initial condition for the temperature is a linear profile between the two walls, whilst the velocity is initially static. Gaussian noise is added to the initial temperature and velocity fields to trigger turbulence in the system. The magnitude of the applied noise is 10^{-8} relative to the initial profiles. The Rayleigh number is set to 1.7×10^5 whilst the Prandtl number is $Pr = 1$. A domain size of $10H \times H \times 10H$ captures the large-scale circulating motions within the system, whilst a mesh of size $480 \times 161 \times 480$ ensures the smallest length scales are well-resolved. A timestep of $\Delta t = 10^{-3}\frac{H}{U_{ff}}$ is used. In total four Simulations have been conducted for the Hartmann number values $Ha = 0, 16, 32, 64$.

4. RESULTS

The simulations begin by going through an initial transient period where the instability occurs, and the initially static fluid begins to flow. Once this transient had passed, statistics were gathered describing the long-term behaviour of the velocity, temperature and current fields. The averaging was done both in time and spatially over the periodic directions. The temperature mean and root-mean-square (RMS) fluctuation can be seen in Figure 1. As the Hartmann number is increased the mean temperature profile tends towards the purely conductive linear profile. The fluctuation of the temperature is higher towards the centre of the cell for moderate values of the Hartmann number. For higher values of the Hartmann number the temperature fluctuation is damped throughout the whole extent of the cavity.

Figure 1. Mean temperature (left) and RMS temperature fluctuation (right) plotted as a function of y.

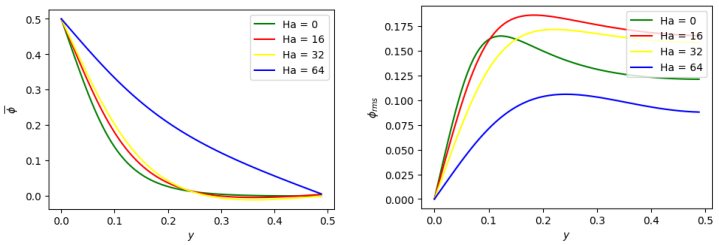

The mean velocity in the system is zero for all three components – this is expected due to the symmetry of the system. The long-term behaviour of the velocity is dominated by its fluctuating component. For the wall-normal velocity, the turbulence is most intense at the centre of the cell whilst for the other components it is most significant nearer to the wall. As expected, the MHD effects damped the turbulence in the velocity field and this effect is more significant as the Hartmann number is increased.

Conducting a similar analysis to [1,2], a posteriori check comparing the mesh-spacing and time-step with the Kolmogorov microscales was conducted confirming that the flow was well resolved for all values of $\{Ra, Pr, Ha\}$. The highest mesh requirements are for $Ha = 0$, indicating that the purely hydrodynamic mesh can be used for the MHD case too. Additionally, the convergence of the results was checked by comparing empirical correlations for the Nusselt number, which can be derived directly from the transport equations. Again, acceptable levels of convergence were shown for all parameter values.

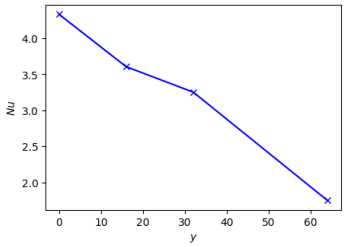

Figure 2. Nusselt number plotted as a function of Hartmann number.

Using the computed values of the Nusselt number, the heat transfer correlation is plotted showing $Nu = Nu(Ha)$. A negative linear trend is observed between Nu and Ha (see fig. 2), which represents the degradation of the heat transfer performance as the magnetic field strength is increased. This is expected, as it is seen in previous MHD simulations [3]. The thickness of the thermal boundary layer is commonly defined as $\delta_b = \frac{1}{2Nu}$ suggesting that the boundary layer increases in size with Hartmann number. This further supports the observation that the resolution requirements of the flow are most significant for $Ha = 0$.

5. CONCLUSIONS

Natural convection of a conducting fluid through a magnetic field has been directly simulated. The action of the magnetic field was to damp the fluctuating velocity whilst causing the mean temperature to tend towards a linear conductive profile. The resolution of the flow was ensured by comparing mesh spacing with Kolmogorov length scales whilst also ensuring that empirical correlations for the Nusselt number are satisfied.

Upcoming work will look to simulate a broader range of the relevant parameters, $\{Ra, Pr, Ha\}$. In particular, these values will include higher values of Ra as well as the fusion-relevant $Pr = 0.025$ and $Pr = 5.25$ corresponding to lithium-lead eutectic and molten salt breeder materials respectively. With this extra data, the more general heat transfer correlation can be calculated, $Nu = Nu(Ra, Pr, Ha)$. Additionally, the effect of magnetic field orientation as well as time-varying and non-uniform fields will be explored.

ACKNOWLEDGMENTS

The authors would like to thank EPSRC for the computational time made available on the UK supercomputing facility ARCHER/ARCHER2 via the UK Turbulence Consortium **(EP/R029325/1).**

REFERENCES

[1] Togni R, Cimarelli A, De Angelis E. Physical and scale-by-scale analysis of Rayleigh–Bénard convection. Journal of Fluid Mechanics 2015;782:380–404. doi:10.1017/jfm.2015.547.

[2] Fregni A, Angeli D, Cimarelli A, Stalio E. Direct numerical simulation of natural, mixed and forced convection in liquid metals: Selected results. Nuclear Engineering and Design 2022;389:111597. doi:10.1016/j.nucengdes.2021.111597.

[3] Yamamoto Y, Kunugi T. Direct numerical simulation of MHD heat transfer in high Reynolds Number Turbulent Channel flows for Prandtl number of 25. Fusion Engineering and Design 2015;90:17–22. doi:10.1016/j.fusengdes.2014.10.005.

[4] Wilson DR, Craft TJ, Iacovides H. Application of Rans turbulence closure models to flows subjected to electromagnetic and buoyancy forces. International Journal of Heat and Fluid Flow 2014;49:80–90. doi:10.1016/j.ijheatfluidflow.2014.04.003.

[5] Bartholomew P, Deskos G, Frantz RAS, Schuch FN, Lamballais E, Laizet S. Xcompact3D: An open-source framework for solving turbulence problems on a Cartesian mesh. SoftwareX 2020;12:100550. doi:10.1016/j.softx.2020.100550.